1966-08

Investigation of noise analysis techniques for the MIT heavy water lattice

Hauck, Frederick Hamilton

Massachusetts Institute of Technology

INVESTIGATION OF NOISE ANALYSIS TECHNIQUES FOR THE MIT HEAVY WATER LATTICE

Frederick Hamilton Hauck

SM Thesis

August 1966 Course 22

INVESTIGATION OF NOISE ANALYSIS TECHNIQUES FOR THE MIT HEAVY WATER LATTICE

by

Frederick Hamilton Hauck

B.S., Tufts University

(1962)

SUBMITTED IN PARTIAL FULFILLMENT
OF THE REQUIREMENTS FOR THE
DEGREE OF MASTER OF
SCIENCE
at the
MASSACHUSETTS INSTITUTE OF
TECHNOLOGY
August, 1966

Signature of Author_____
Department of Nuclear Engineering

Certified by_____
Thesis Supervisor

Certified by_____
Thesis Supervisor

Accepted by_____
Chairman, Departmental Committee
on Graduate Students

INVESTIGATION OF NOISE ANALYSIS TECHNIQUES FOR THE MIT HEAVY WATER LATTICE

by

Frederick Hamilton Hauck

Submitted to the Department of Nuclear Engineering on August 22, 1966, in partial fulfillment of the requirements for the degree of Master of Science in Nuclear Engineering.

ABSTRACT

A reliable system for performing a Fourier analysis of a reactor noise signal has been constructed and utilized. Both auto- and cross-correlation techniques were used to study noise signals from the MITR hohlraum and the exponential lattice. As predicted by theory, the efficiency of the detectors used was insufficient to provide positive results. The lattice transfer function was electronically simulated and analyzed by the system confirming the reliability of the equipment.

Several methods are suggested for increasing detector efficiencies to provide signal levels which will permit extraction of information about the kinetic behavior of the test lattice.

Thesis Supervisor: Dr. F.M. Clikeman
Title: Assistant Professor of Nuclear Engineering

Thesis Supervisor: Dr. M.J. Driscoll
Title: Assistant Professor of Nuclear Engineering

ACKNOWLEDGEMENTS

The author wishes to express sincere thanks to all those persons who have given assistance during the course of this work. Mr. David Gwinn has provided invaluable advice in the construction and testing of the equipment. Messrs. Joseph Barch, Norman Berube, and Albert Supple have been of considerable help in setting up the lattice instrumentation. Digital computation was done at the MIT Computation Center.

The author appreciates having had the opportunity to work under his thesis supervisors, Dr. M.J. Driscoll and Dr. F.M. Clikeman, whose assistance and encouragement have been essential to its success.

The author is especially grateful to the Office of Naval Research, whose sponsorship enabled him to participate at MIT in the U.S. Navy's Advanced Science Program.

Finally, the author is indebted to his wife, Dolly, who contributed invaluable moral support.

TABLE OF CONTENTS

LIST OF FIGURES

LIST OF TABLES

CHAPTER 1

INTRODUCTION

1.1 Background

In studying the neutron characteristics of any nuclear reactor core assembly it is desirable that the research be done as economically as possible, and preferably that several independent methods be used to determine the desired information. The MIT Lattice Research Project has for some time studied various reactor parameters in a heavy water-moderated exponential facility located adjacent to the MIT Reactor.[1-5] See Figure 1.1 for a cut-away view of the MIT Lattice Research Facility.

In recent years, considerable use has been made of the pulsed neutron technique in determining k_∞ for test lattices in order to provide data supplementing the more common static parameter measurements.[6] It is the purpose of this thesis to explore the utility of the noise analysis technique as a means of complementing the pulsed neutron and other methods of measuring the various parameters measured in the MIT heavy water lattices.

1.2 Noise

The term "noise" refers to the random or stochastic fluctuations in the output signal from a system. Reactor noise is thus the random fluctuation of power level due to the discrete nature of the multiplication process. These fluctuations are generally small, and usually only about one percent of the total power level. In order to observe this noise, a detector must be used and often

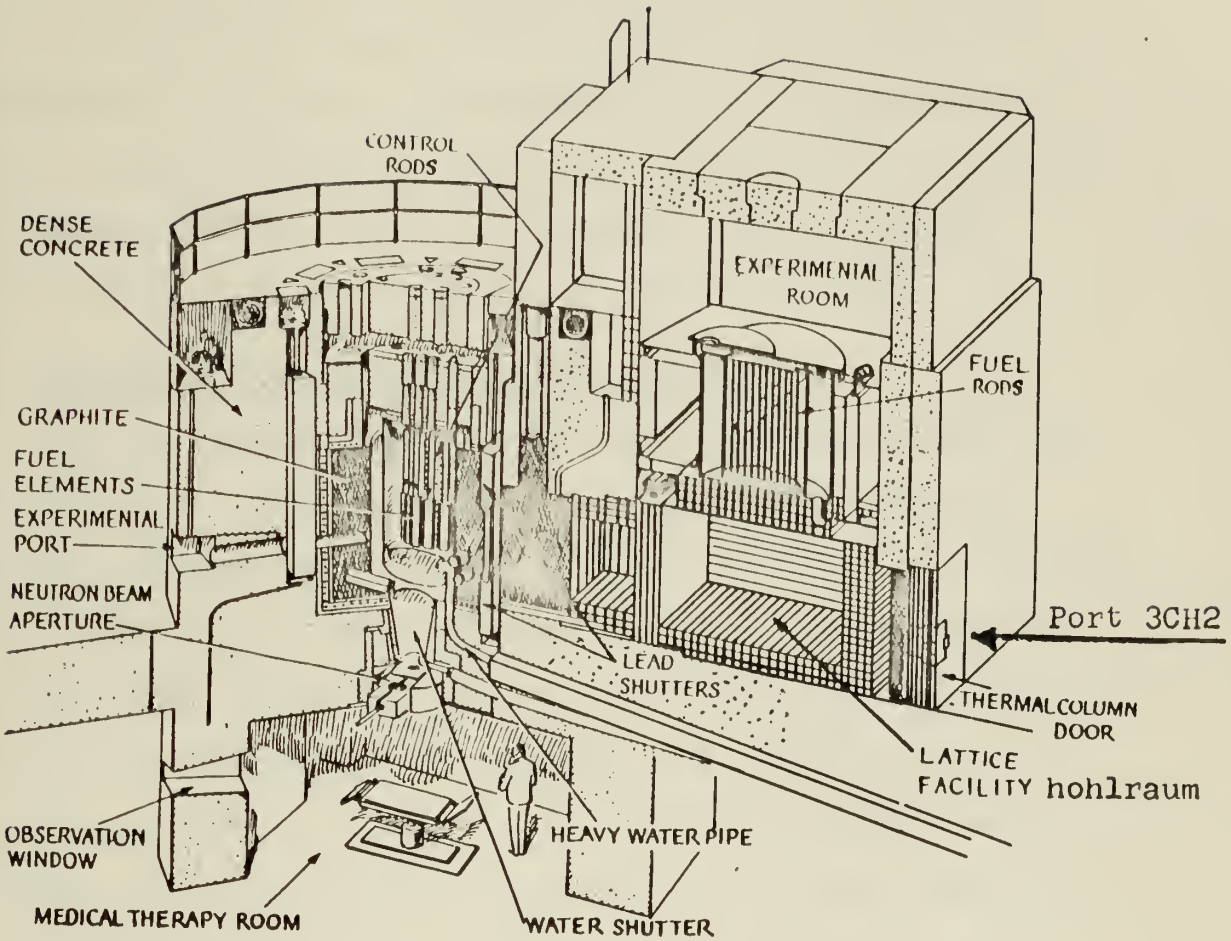

Fig. 1.1 Cut-away View of MIT Lattice Research Facility

the term reactor noise is used to describe the fluctuations of the output signal of the detector. It is important to remember, however, that the detector only sees a token sample of these fluctuations and that, owing to the finite size of the detector, the spatial-dependence of the noise measurement is blurred. Only recently has the space-dependence of reactor noise been closely examined.(7) Throughout this paper, however, space-independence will be assumed since this will prove adequate for present purposes.

1.3 Summary of Theoretical Considerations

Since a reactor depends upon neutron multiplication for its operation, it is reasonable to expect that among the various neutrons which are registered by a detector, many which have a common ancestry will produce pulses superimposed upon the d.c. level of the signal. The number of such related pulses will depend upon the detector efficiency as will be seen later. While the detector d.c. level is itself maintained by the accumulation of many pulses, we are unable to extract any information involving the discreteness of the multiplication process from it, and it thus holds no interest for us here. Thus one can instead focus attention upon a fluctuation in the signal due to the daughter neutron of a given fission, followed a certain Δt later by another impulse due to a grandaughter neutron of the same fission. Since this time interval Δt is a function of the neutron lifetime in a given system, it should be possible to extract information about the multiplying properties of the medium

by submitting the a c (or noise) portion of the detector signal to analysis. One method of analysis is to determine the autocorrelation function, which is defined as the expectation value of the product of the signal at a time t_1, and the signal at a time t_2:

$$\phi_{nn}(\tau) = E\left[n(t_1)n(t_2)\right] \quad (1.1)$$

where for simplicity the signal is taken to be the neutron density n(t), and $\tau = t_1 - t_2$. Following the development of Bierman, et al.,[8] one can evaluate $\phi_{nn}(\tau)$ by first considering the standard reactor kinetics equations in their space-independent, linear, time-invariant form:

$$\frac{dn}{dt} = \frac{k(1-\beta)-1}{\ell} n + \sum_i \lambda_i C_i + S \quad (1.2)$$

$$\frac{dC_i}{dt} = -\lambda_i C_i + k \frac{\beta_i}{\ell} n \quad (1.3)$$

Since only prompt neutron behavior is of importance, these equations may be put in the form:

$$\frac{dn}{dt} + \alpha n = k \frac{\beta}{\ell} n_o + S = f(t) \quad (1.4)$$

where $\alpha = \frac{1-k(1-\beta)}{\ell}$, the prompt neutron decay constant, and the inhomogeneous terms are considered as the forcing function f(t).

The solution to Eq. (1.4) may be written as a convolution integral:

$$n(t) = \int_{-\infty}^{\infty} W(t-\tau) f(\tau) d\tau \quad \int_0^{\infty} W(\tau) f(t-\tau) d\tau \quad (1.5)$$

where $W(t-\tau)$ is the impulse response function of the system. This function is obtained by normalizing the homogeneous solution to Eq. (1.4) and is found to be:

$$W(t-\tau) = \begin{cases} \alpha \exp[-\alpha(t-\tau)] & t > \tau \\ 0 & t < \tau \end{cases} . \qquad (1.6)$$

One may evaluate Eq. (1.1) giving:

$$\phi_{nn}(\tau) = \frac{\alpha}{2} e^{-\alpha\tau} . \qquad (1.7)$$

If one were to assume that the forcing function were instead a burst of neutrons, as in a pulsed neutron experiment, $f(t)$ could be approximated by a Dirac delta $\delta(t)$ giving as a solution to Eq. (1.4):

$$n(t) = \alpha e^{-\alpha t} .$$

At this point, the complimentary nature of the pulsed neutron and noise analysis experiments becomes evident, for each provides an independent method for determining the prompt neutron decay constant α.

Various noise analysis methods are available for determining α by studying the a.c. detector signal in the time domain,[9] however, by transforming Eq. (1.5) into the frequency domain by the use of Fourier transforms, a method of analysis which involves less data processing can be employed.

The Fourier transform of the autocorrelation function is called the power-spectral-density function and is given by:

$$\Psi_{nn}(\omega) = \frac{1}{\pi} \int_{-\infty}^{\infty} \phi_{nn}(\tau) e^{-j\omega\tau} d\tau . \qquad (1.8)$$

which when combined with Eq. (1.7), gives:

$$\Psi_{nn}(\omega) = \frac{\alpha^2}{\pi}\left[\frac{1}{\alpha^2+\omega^2}\right] \qquad (1.9)$$

The spectral shape of Eq. (1.9) is that of a low pass filter with a breakpoint at $\omega = \alpha$. Thus, if a Fourier analysis of the detector signal is performed, it should be possible to determine α, the prompt neutron decay constant.

1.4 Detector Efficiency

In order to compare the utility of the pulsed neutron and noise measurements, Rieman et al [6] noted that both experiments are hampered by other spurious signal levels. In the pulsed neutron experiment, these take the form of residual neutron levels due to the neutron sources in the system, and can be overcome by increasing pulse intensity. In noise experiments, as we shall see in this section, the detection process itself provides a white background power spectrum, which can only be overcome by increasing detector efficiency or by performing cross-correlation experiments. These limitations can be described by including the background as an additive constant to both expressions:

$$N(t) = A_p + B_p e^{-\alpha t} \qquad (1.10)$$

$$\Psi_{nn}(\omega) = A_n + \frac{B_n}{1+\omega^2/\alpha^2} \qquad (1.11)$$

where now a figure of merit for each system can be defined as:

$$\frac{B}{A+B}\ .$$

The utility and feasibility of noise experiments thus depends upon the magnitude of the figure of merit

By pursuing the analytical method of Cohn[10], and extending it to the case of a subcritical reactor, the effects of detector efficiency can be studied. The basis of this method rests on what is known as the Schottky formula, which was originally developed to describe the noise in a temperature limited electronic diode. It is:

$$\langle |I|^2 \rangle = 2e^2\bar{m} \quad , \tag{1.12}$$

where $\langle |I|^2 \rangle$ is the spectral density of the diode current noise in amps^2 sec, e is the charge carried by each electron in coulombs, and $\bar{m}$ is the average number of electrons flowing per second. Cohn adapts this formula to the reactor case giving:

$$\langle |S_o|^2 \rangle = 2 \sum_i q_i^2 \bar{m}_i \quad , \tag{1.13}$$

where $\langle |S_o|^2 \rangle$ is the spectral density of the noise equivalent source in neutrons^2 sec^{-1}, q_i is the net number of neutrons produced in a nuclear process of type i, and $\bar{m}_i$ is the average number of nuclear processes of type i occurring per second in the reactor. As shown in Appendix A this formulation results in the following expression for the noise equivalent source in a subcritical assembly:

$$\langle |S_o|^2 \rangle = \frac{2n}{\ell} \left[2 - k - \frac{k}{\bar{\nu}} + \frac{k^2}{\bar{\nu}} (\overline{\nu^2} - 2\bar{\nu} + 1) \right] \tag{1.14}$$

This source is transformed by the reactor source transfer function $T(\omega)$ into the neutron spectral density:

$$\langle |n(\omega)|^2 \rangle = |T(\omega)|^2 \langle |B_0|^2 \rangle \qquad (1.15)$$

By considering the power spectral density of the detector current due to both the correlated and uncorrelated neutrons, it can be shown that the total detector current auto-power-spectral-density is:

$$\langle |I_\alpha(\omega)|^2 \rangle = 2Q^2 \epsilon F_0 \left\{ 1 + \frac{\epsilon k_p}{\bar{\nu}} \left[2 - \frac{k_p}{\bar{\nu}} - k_p + \frac{k_p^2}{\bar{\nu}} (\overline{\nu^2} - 2\bar{\nu} + 1) \right] \frac{1}{\omega^2 + \alpha^2} \right\}, \qquad (1.16)$$

where

ϵ = detector efficiency = $\frac{\text{fissions detected}}{\text{fissions occurring}}$

F_0 = fission rate = $\frac{k_0 n}{\bar{\nu} \ell}$

$k_p = k(1-\beta)$

$\bar{\nu}$ = average number of neutrons emitted per fission

Q = charge collected per fission detected

$|T(\omega)|^2 = \frac{1}{\omega^2 + \alpha^2}$

Thus, for an autocorrelation measurement, the detector efficiency must be such that the right-hand term is greater than unity, or for $\omega \ll \alpha$:

$$\epsilon \geq \frac{\bar{\nu}}{k_p} \frac{(1-k_p)^2}{\left[2 - \frac{k_p}{\bar{\nu}} - k_p + \frac{k_p^2}{\bar{\nu}} (\overline{\nu^2} - 2\bar{\nu} + 1) \right]} \qquad (1.17)$$

Using the accepted values[9] of 2.5 for the factor $\bar{\nu}$ and 7.47 for $\overline{\nu^2}$, this becomes:

$$\epsilon \geq \frac{6.25(1-k_p)^2}{k_p \left[5 - 3.5\, k_p + 3.47\, k_p^2 \right]} \qquad (1.18)$$

Figure 1.2 displays this restriction for $k \leq 0.90$.

Since detector efficiencies above 10^{-2} are very difficult to obtain without significantly disturbing the system under study, a major stumbling block to the use of noise analysis in far-subcritical systems ($k < 0.9$) becomes obvious. Some of this problem could be alleviated if the uncorrelated noise is filtered out. By using two detectors and multiplying the a.c. components of their signals, those pulses which did not coincide would tend to cancel out whereas those which did coincide would reinforce each other and, over a period of time, the correlated portion of the spectrum would tend to be emphasized. This method of cross-correlation was used by Seifritz, Stegemann, and Väth in making measurements on the coupled fast-thermal reactor STARK.[11] Their results indicated that with their equipment, a ratio of correlated to uncorrelated noise of 0.1 was sufficient to give meaningful results if cross-correlation techniques were used. This is a factor of twenty improvement over the ratio of 2 which they needed in auto-correlation experiments. Of course, the relative advantage of cross-correlation over auto-correlation experiments depends upon the individual analysis equipments and how the signal is analyzed. Figure 1.1 shows the cross-correlated detector efficiencies required based on their experience. Notice that detector efficiencies of close to one percent are still required for a k of 0.7 to 0.8, which is the range of primary interest in MIT lattice facility work.

1.5 Purpose of Present Work

This thesis is concerned with, after assembling a reliable analysis system to perform both auto- and

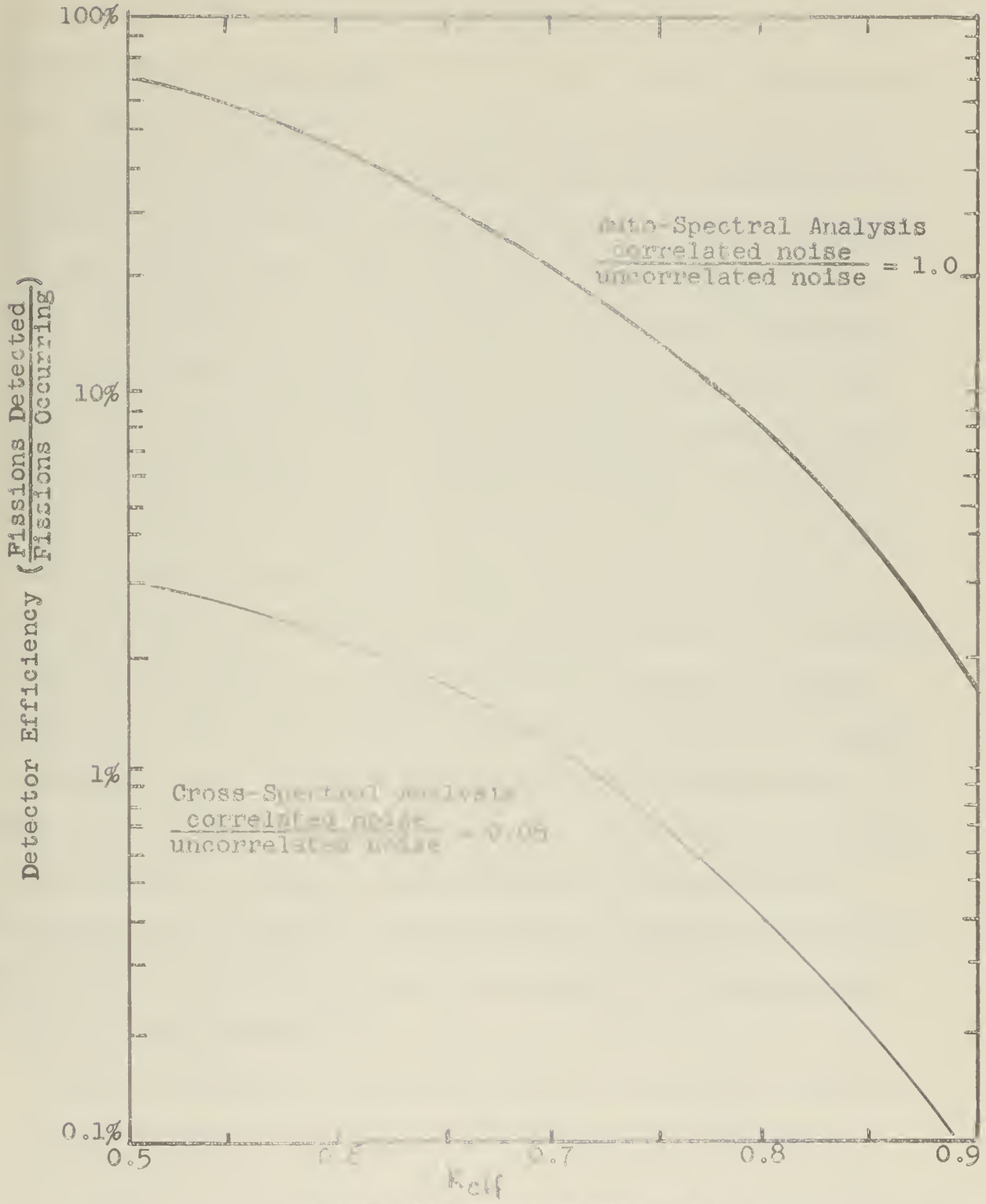

Fig. 1.2 Detector Efficiency required vs. k_{eff} for Noise Spectral Analysis

cross-correlation spectral measurements. From the start, it was realized that once such a system were constructed, the problem of attaining sufficiently large detector efficiencies would have to be solved.

Detector efficiency is purely a matter of detector size and neutron sensitivity. Of all detectors readily available, the Westinghouse Type 6377 ionization chamber provided the best combination of neutron sensitivity (4×10^{-14} amperes/neutron/cm^2/sec) and size (100 cm^2 of sensitive area). As such, this detector was still not efficient enough (in the hohlraum and lattice, $\epsilon \sim 9 \times 10^{-7}$) to measure the spectral density; however it served two purposes. First, it provided a noise signal comparable in size to those which would be studied in the lattice later, and thus provided us with information on the design requirements for the analysis system. Second, any very large resonances in the hohlraum which might be present due to spatial effects might still be detected. Thus, both auto- and cross-correlation measurements were made in the lattice to insure that a reliable system would be available in the future. Concurrently, a separate study was being made of methods for increasing detector efficiencies to the levels needed [12].

Chapter 2 describes the work during the initial phase of system assembly and hohlraum measurements. Chapters 3 and 4 [illegible] by both auto- and cross-correlation techniques. Chapter 5 contains [illegible]

CHAPTER 2

ASSEMBLY OF EQUIPMENT AND PRELIMINARY HOHLRAUM MEASUREMENTS

2.1 Assembly of Equipment

Several methods of analyzing noise signals have been developed, often classified as to whether the analysis is done concurrently with reactor operation, or done afterward by analyzing either an electronically or mechanically (pen-recorder) recorded signal.[9] Whether the analysis is done digitally or continuously, further specifies the method of analysis to be used. The choice of method of course depends upon financial and/or time limitations, and also upon the degree of accuracy desired.

For present purposes, it was decided that the use of analog computing equipment would provide the most flexible system of analysis. Not only would it provide a real-time method of continuous analysis but it would also be adaptable to other uses such as reactor dynamics simulation. For this reason one George A. Philbrick MU/DV Duplex Multiplier/Divider and three G.A.P. Model HK Operational Manifolds (each containing five chopper-stabilized operational amplifiers), were acquired. The latter afford the capability of performing a total of fifteen separate linear operations on one or more signals, whereas the former performs the non-linear operations of multiplying or dividing. (See Appendix D for a brief discussion of the characteristics of operational amplifiers and a description of the basic circuits used in performing the linear operations.) The method of analysis used was to

take the Fourier integral of the auto-correlation function with zero delay time. A block diagram of the circuitry is shown in Figure 2.1.

After using the heterodyning technique of multiplying the detector noise by a sine wave of known frequency, a low frequency band-pass filter of fixed bandwith $\Delta\omega$ is used to pass only those noise components whose frequency differs from that of the oscillator by less than the filter bandwidth. The resulting signal is squared and integrated. Division by the integration time gives the amplitude of the spectral density at a frequency $\omega_o - \Delta\omega$, in a bandwidth $\Delta\omega$. Scanning the spectrum is accomplished by varying the oscillator frequency ω_o over the desired range.

2.2 Preliminary Experimentation

Initial assembly of the equipment and experimentation were done by the author together with A. Diaz-Moreno.[13] As stated earlier, this first phase was to serve two purposes. First to determine if the analyzing equipment was performing correctly, and secondly to determine if the thermal column and hohlraum served as a true white noise source of neutrons. This latter question is important since, as can be seen by Eq. (1.15), determination of the lattice transfer function requires foreknowledge of the spectral density of the source. Only when the external source is itself random may the simplified pile noise formulation be used.[10]

For these measurements, a Westinghouse Model 6377 ionization chamber, was placed in the hohlraum through a hole bored through the graphite wall inside port #30.

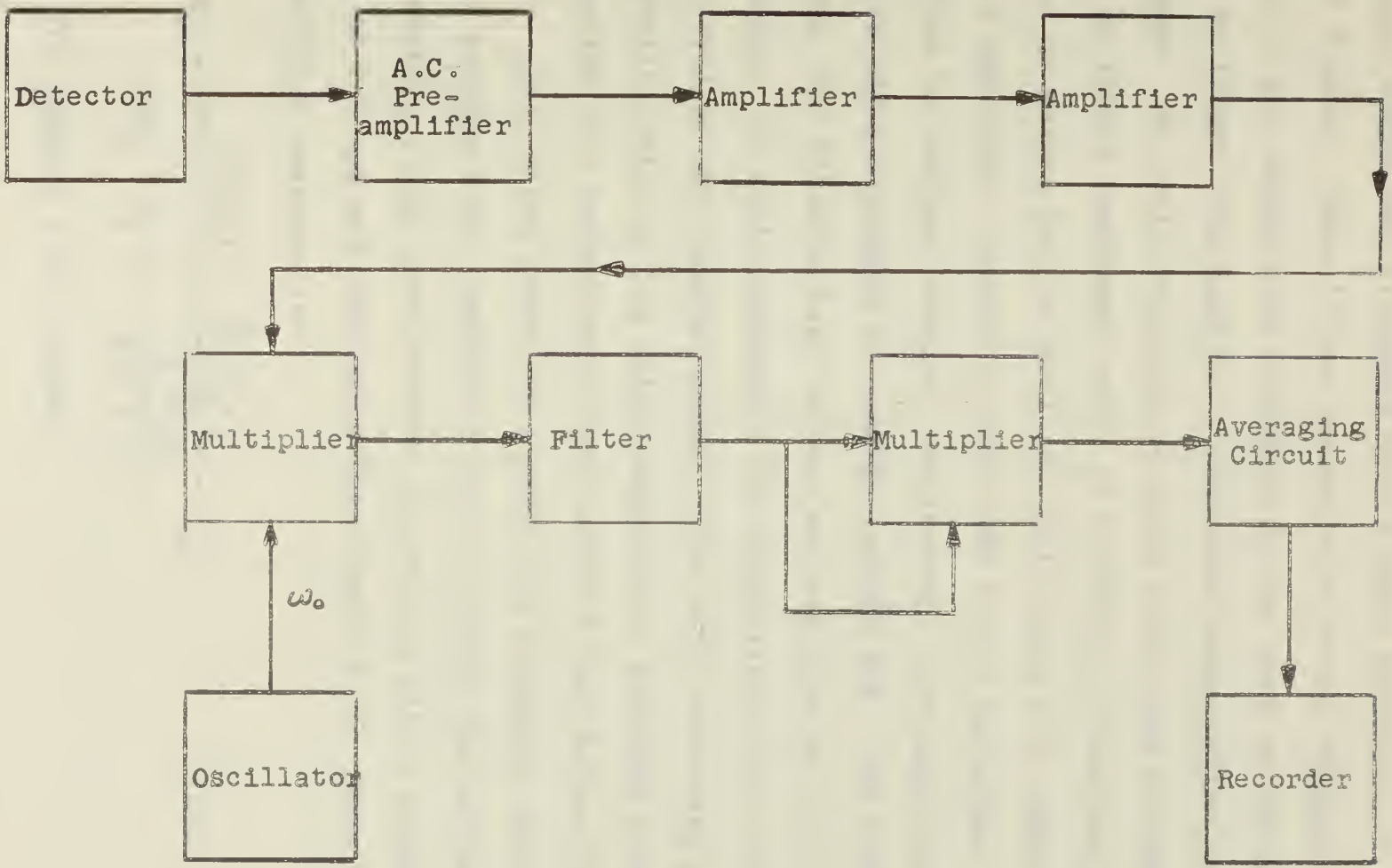

Fig. 2.1 Block Diagram of Auto-Spectral Density Analysis System

Preliminary measurements showed that the total d.c. detector output was 175 μamps with a noise component of about 1 μamp. Since it was desirable to have a voltage input to the vacuum-tube equipment on the order of one-half volt or larger, the need for a high gain preamplifier became apparent. To avoid excessive 60 cycle pickup and to introduce as little instrument noise as possible, it was decided to use an Analog Device Model 106 Solid State A.C. operational amplifier, powered by four F4BP 6 volt batteries. In addition to meeting technical requirements, the amplifier has the added advantage of economy costing $26. For similar reasons, the detector high voltage was supplied by 10 67.5 V batteries. To avoid saturating the preamplifier with the d.c. level of the incoming signal while still obtaining maximum amplification of the noise component, a buckling voltage controlled by a potentiometer was inserted just before the input. Also, since there was a large low frequency variation in the neutron flux, apparently due to control rod motion in the reactor, a high pass network (R_2 and C_2) with a breakpoint at 2.5 cps was introduced (see Figure 2.2). Thus the preamplifier response is:

$$e_o = \frac{-2R_2R_1\left(1 + \frac{1}{2}R_2C_2s\right)}{(2R_2 + R_1)\left(1 + \frac{R_2{}^2C_2s}{2R_2 + R_1}\right)} i_{in} \qquad (2.1)$$

which for large $s = j\omega$ becomes

$$\frac{e_o}{i_{in}} = -R_1 . \qquad (2.2)$$

Although a high frequency roll-off due to finite space charge

R_1 = 510 KΩ
R_2 = 12 KΩ
C_2 = 220 μf
R_3 = 100 KΩ
P_1 = 500 KΩ
E = -12 V
A = 150,000

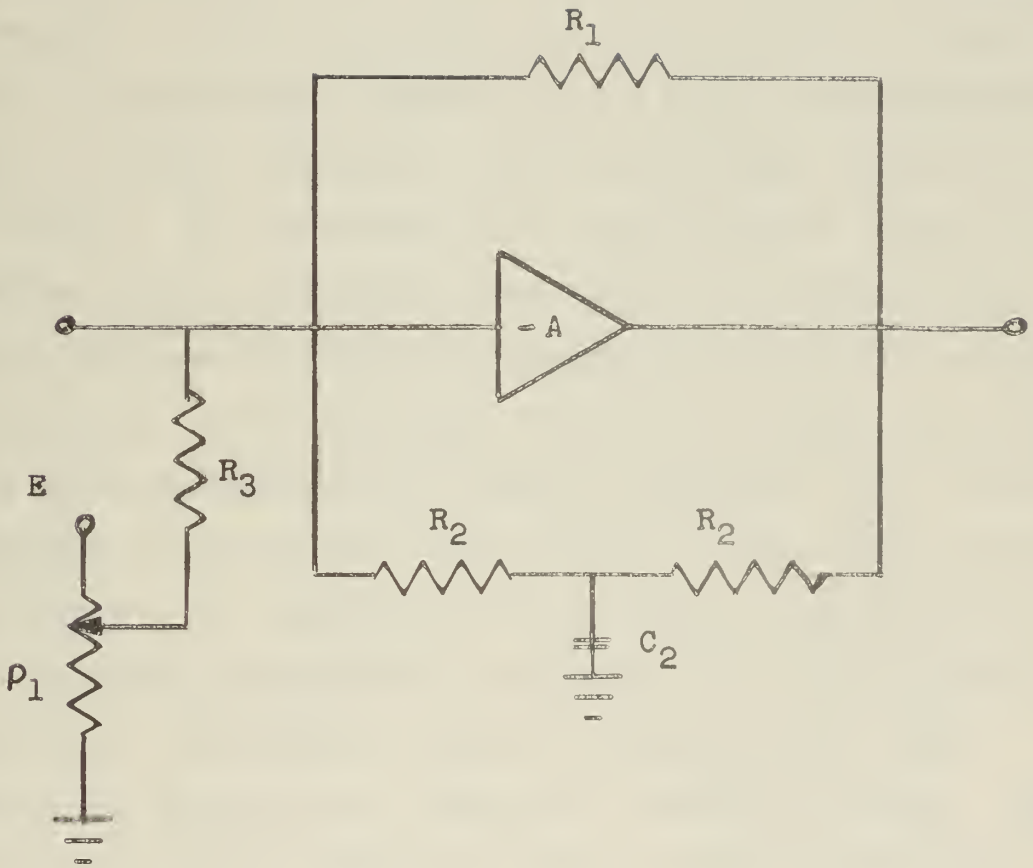

Fig. 2.2 High Gain A.C. Preamplifier Circuit

collection times was observed, the preamp-detector frequency response was constant up to 5,000 cps for a detector voltage of 720 V.

The noise amplitude at the preamp output was about one-half volt, which was sufficiently large compared to the 0.01 V self-noise of the preamp. Two stage amplification with a total gain of 200 provided a 100 V peak-to-peak signal at the input to the heterodyning multiplier. Here, the signal is multiplied by a 100 V peak-to-peak sine wave of known frequency. Since the output of the multiplier is scaled by 100 V, the resultant signal is 100 V p-p. The combination of the two filters produced a 0.88 cps pass-band centered at 0.128 cps. The inclusion of an amplifier with a gain of 20 between filters maintained the signal at a sufficiently high level to make the effects of component drift at this stage negligible. After squaring, the filtered signal was integrated using an averaging or "leaky" integrator, with a time constant of 100 seconds. The circuit at this point is shown in Figure 2.3. Results of the preliminary measurements in the hohlraum are presented in Figure 2.4. Two features are important. The first, already described, is the high frequency roll-off as a function of detector voltage. The second is the low frequency erratic peaking in amplitude.

To investigate the latter, the effect of the reactor source neutrons was considered. Since these neutrons originate in the critical MIT Reactor, a low frequency breakpoint in the reactor neutron spectral dens[illegible] would be expected at $\omega = \beta/\ell$. This value is approximately .0075/.0015 for the

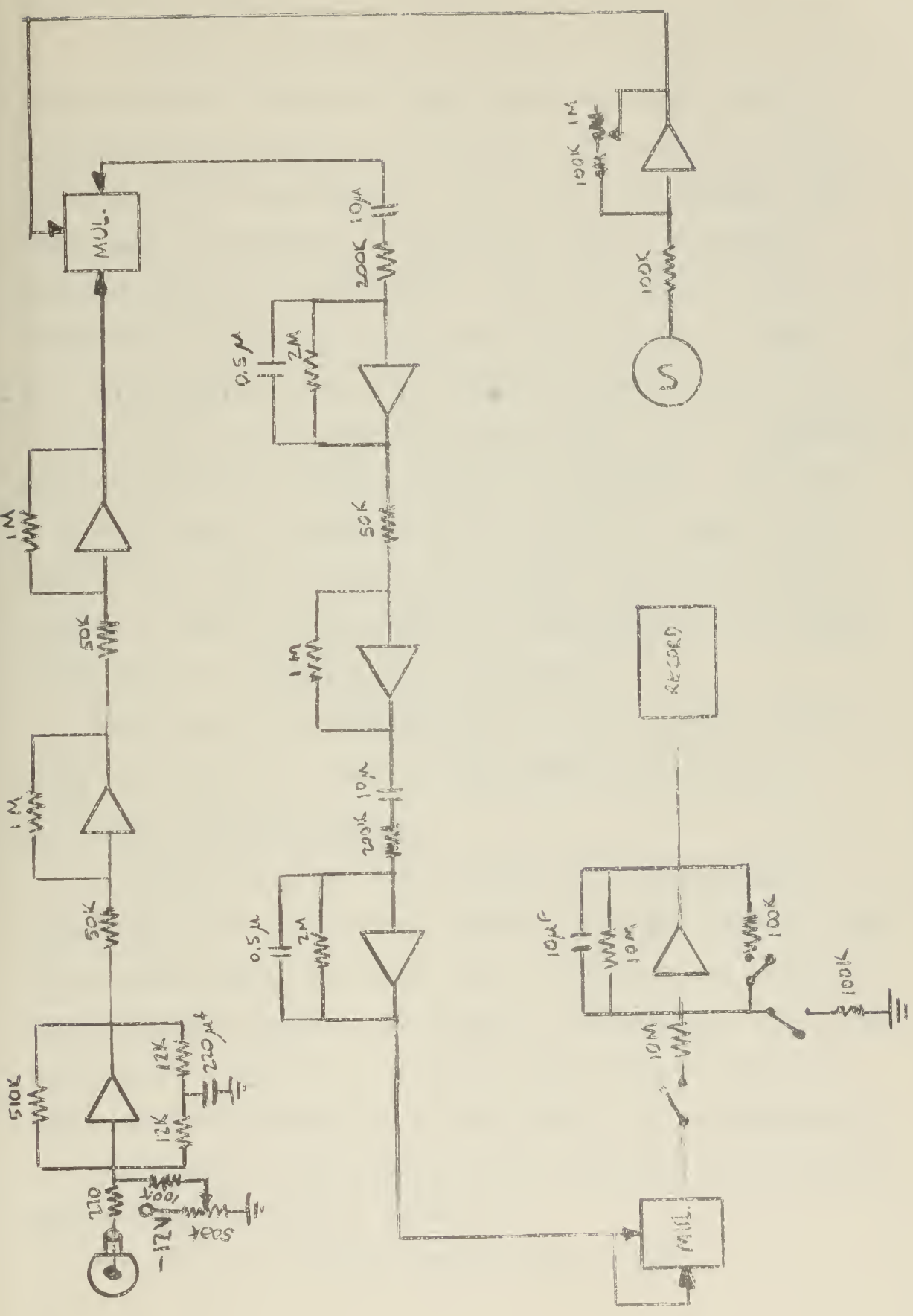

Fig. 2.3 Circuit Diagram for Auto-Spectral Density Measurements

MIT Reactor, resulting in a break at $f = \alpha/2\pi = 0.796$ cps.

In order to determine the amount of correlation introduced into the lattice by these source neutrons, one can assume that the lattice is a detector and apply Eq. (1.16). To do this, the efficiency of the lattice for reactor neutrons must be estimated. Less than 0.02% of the reactor neutrons pass the hohlraum.[14] This value may be taken as an upper limit for the efficiency of the lattice. Using Eq. (1.16) for the case of a critical reactor ($k \lesssim 1$), with $\alpha = 4.8$ sec^{-1}, it is seen that above about 5 cps, correlation of neutrons in the lattice should be negligible. Since the frequency range of interest in the lattice is about 3,000 cycles, the effect of the low frequency correlation may be ignored. Thus the hohlraum may be considered to be a white noise source of neutrons for the lattice.

For this reason, ~~this~~ the behavior of the spectral density curve of Figure 2.4 below 100 cps caused some concern.

2.3 First Phase Conclusions

In order to check on the reliability of the system, measurements of the spectral density were taken several times on different days. Above 50 cps, the results were found to be reproduceable within the predicted experimental error (see Appendix D). Scattering of data points below 50 cps cast doubt upon the reliability of the system at low frequencies.

Preliminary investigations were concluded at this point with the next objectives being to:

a) attempt to improve detector efficiency

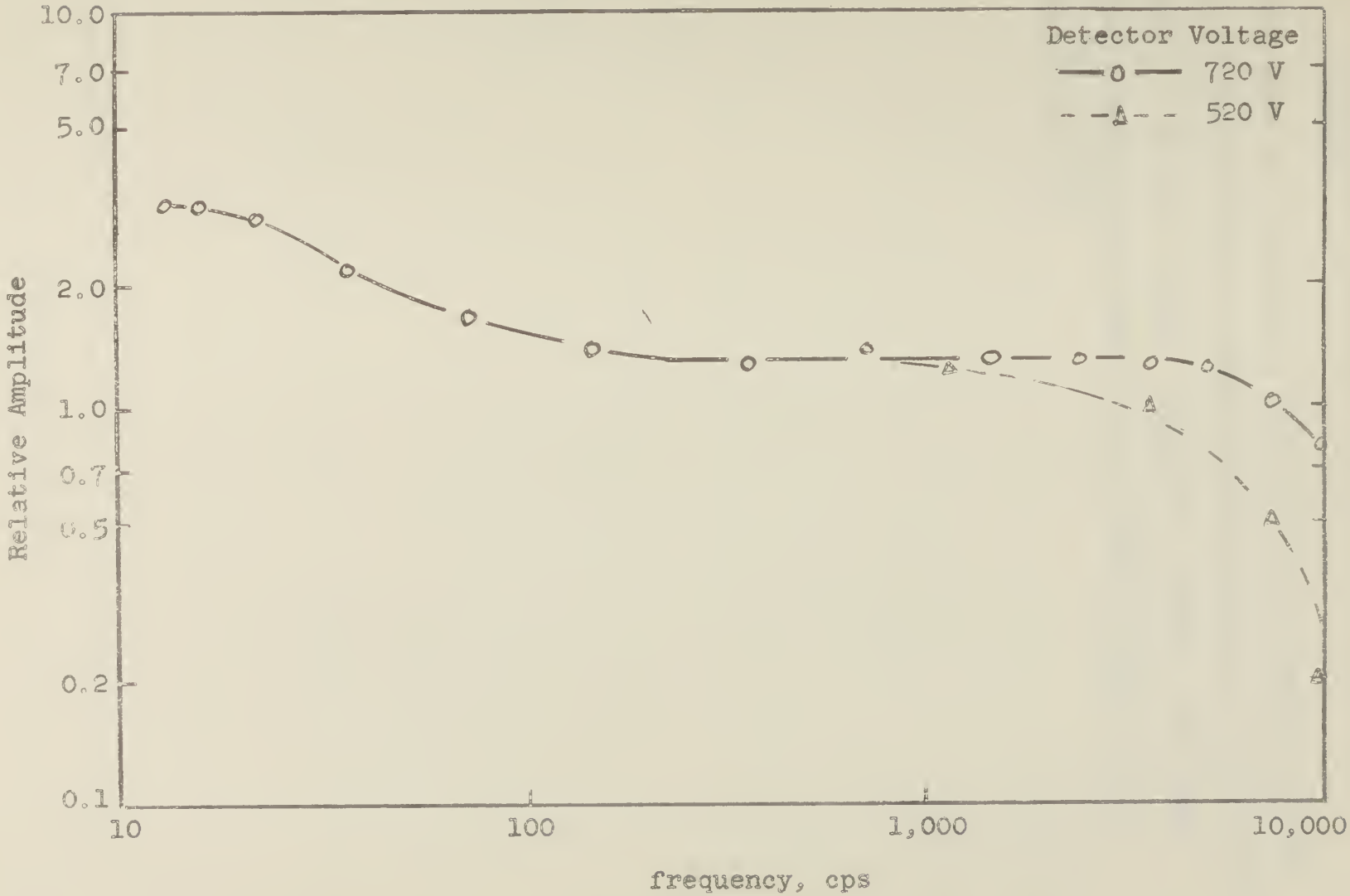

Fig. 2.4 Results of Preliminary Hohlraum Auto-Spectral Density Noise Measurements

b) investigate more thoroughly the low frequency response of the system

c) investigate frequency response in the lattice itself.

The problems of developing a detector with increased efficiency for lattice noise analysis is the subject of another SM thesis[12] by M.G. Johnson, currently underway. The next chapter describes work done by the present author on the items (b) and (c).

CHAPTER 3

LOW FREQUENCY TESTS AND AUTOCORRELATION MEASUREMENTS

Section 2.3 described the erratic behavior of the analyzer at low frequencies. It was necessary to determine the cause of this behavior before proceeding to lattice autocorrelation measurements.

3.1 Introduction

Up to this point, the oscillator signal had been provided by first a General Radio Unit R-C Oscillator Type 1210-C and later a Hewlett Packard Test Oscillator, Model 650A, the latter providing the signals of lowest frequency down to 10 cps. In order to look more closely at the low frequency response, a Waveforms Model 403B oscillator was used, providing signals as low as 1 cps. The filters were also modified as shown in Figure 3.1.

This time the spectral density of the hohlraum noise was investigated in the range 1 to 200 cps, with the results shown in Figure 3.2. As can be seen, results were again erratic, with a general trend of higher amplitudes at lower frequencies.

The erratic low frequency response suggested the possibility of component drift, while the increase in amplitude at low frequencies suggested that the d.c. portion of the detector signal was not being completely cancelled, allowing the carrier wave to be passed to the filters. Referring to the latter problem, note that a one-half volt d.c. signal at the noise input to the multiplier, when multiplied by a 100 V peak-to-peak carrier signal, of frequency ω_0 will result in

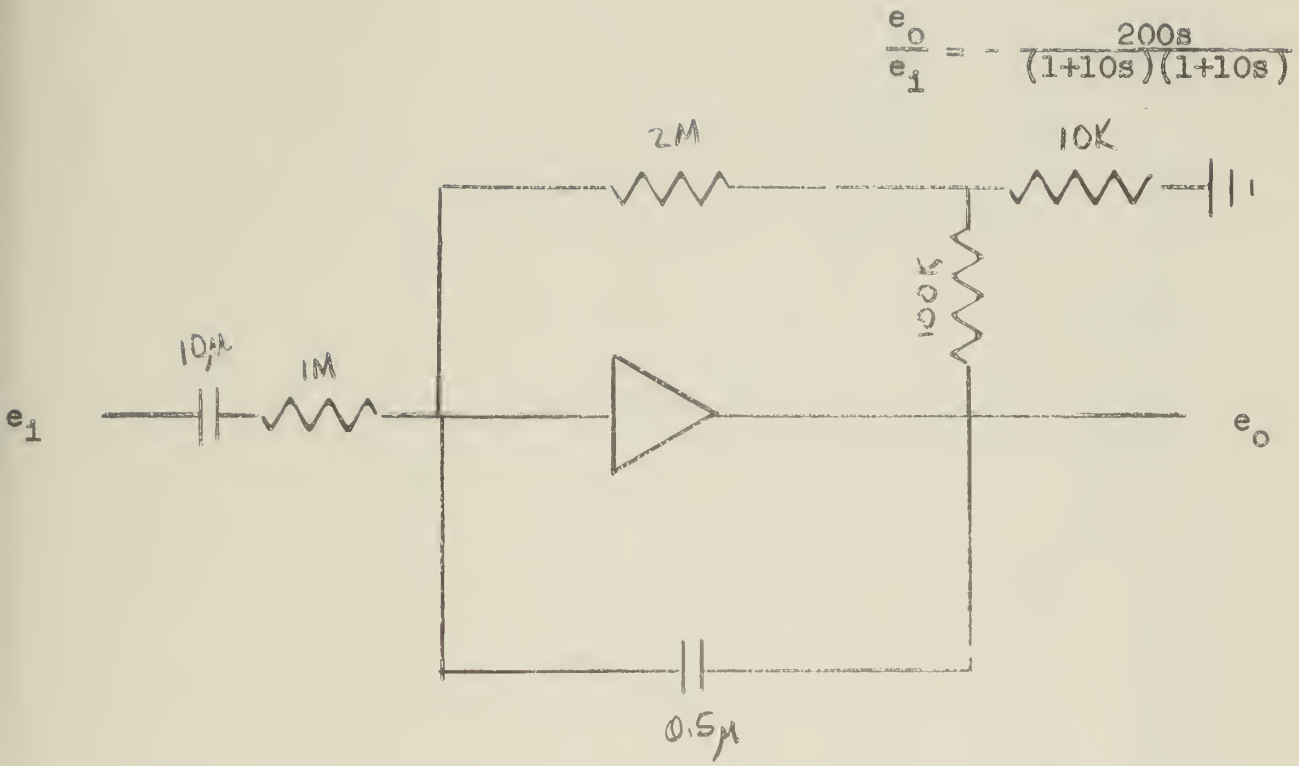

Fig 3.1 Filter Modifications to Allow Low Frequency ~~Modifications~~ Measurements.

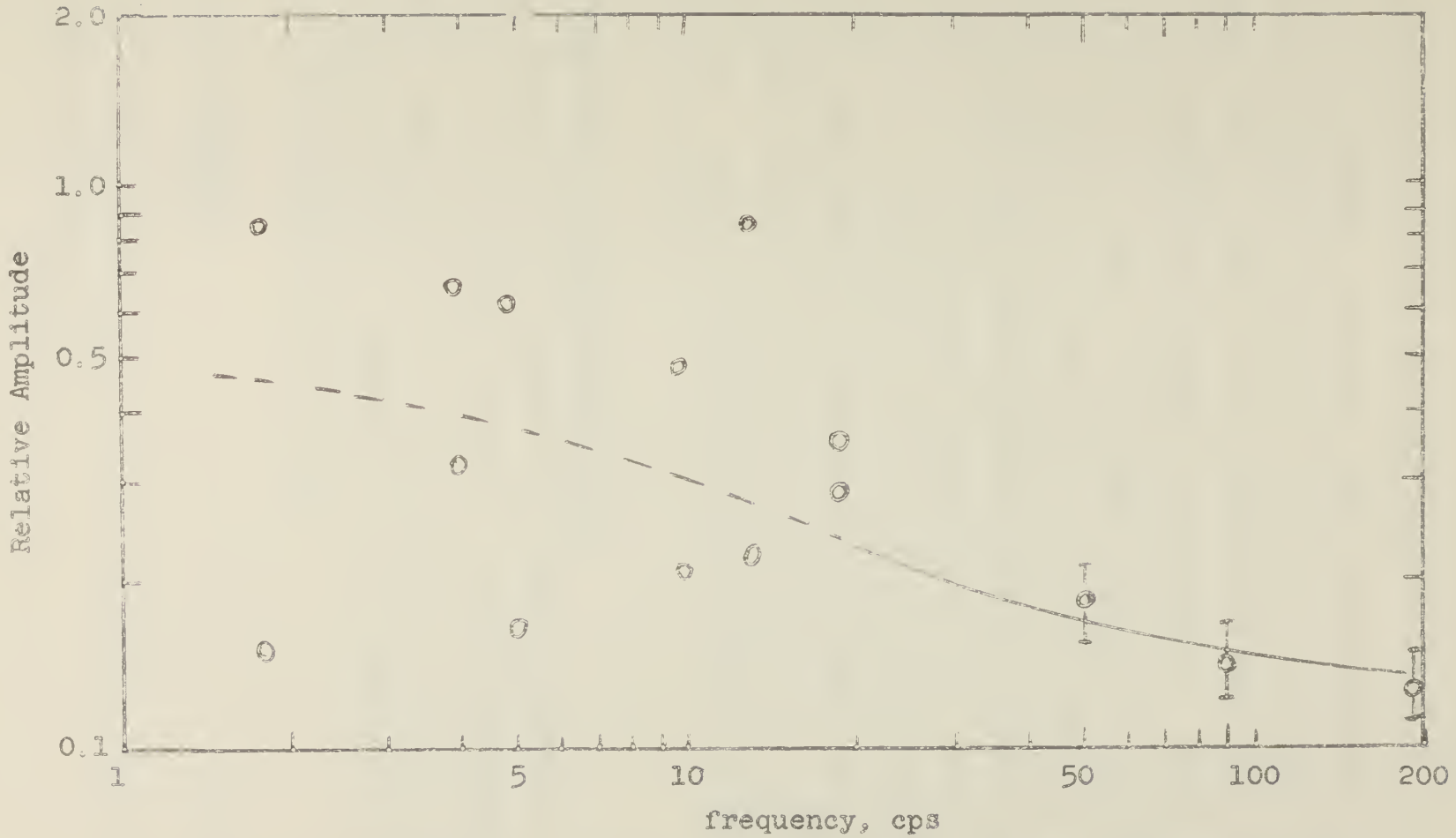

Fig. 3.2 Initial Low-Frequency Hohlraum Measurements. Data points are random samples merely to show range ~~in~~ of values measured

a one-half volt peak-to-peak sine wave at the multiplier output. At high frequencies (such that ω_o is much greater than the center frequency of the filter) this component is filtered out leaving only the signal due to the a.c. (noise) portion of the signal. However, since the filters are not square (effectively 24 db/octave attenuation as seen at the averaging circuit input), at low frequencies this sine wave would not be attenuated enough to be negligible. Total cancellation of the d.c. level of the signal was insured by adding a blocking capacitor in series with the first amplifier.

Multiplier drift (rated at ±1%) which was measured to be as much as 2 V in one hour, accounted for the erratic behavior at low frequencies. This drift was minimized by adding a ventilating fan to provide better temperature stability; however, drifts of up to 0.75 V per hour were still encountered. Figure 3.3 shows how these measures served to reduce these problems.

3.2 Simulation of Lattice Measurement

To insure that the equipment was indeed operating properly, it was decided to simulate a lattice measurement by adding a capacitor to the preamplifier, in parallel with the feedback resistor. Neglecting the low frequency filter network, the preamplifier has a gain:

$$\frac{e_o}{i_n} = \frac{R_f}{1 + R_f C_f s} \quad . \tag{3.1}$$

With R_f = 510K (1%) and C_f = .001 μf, (measured) this results in a simulated breakpoint at:

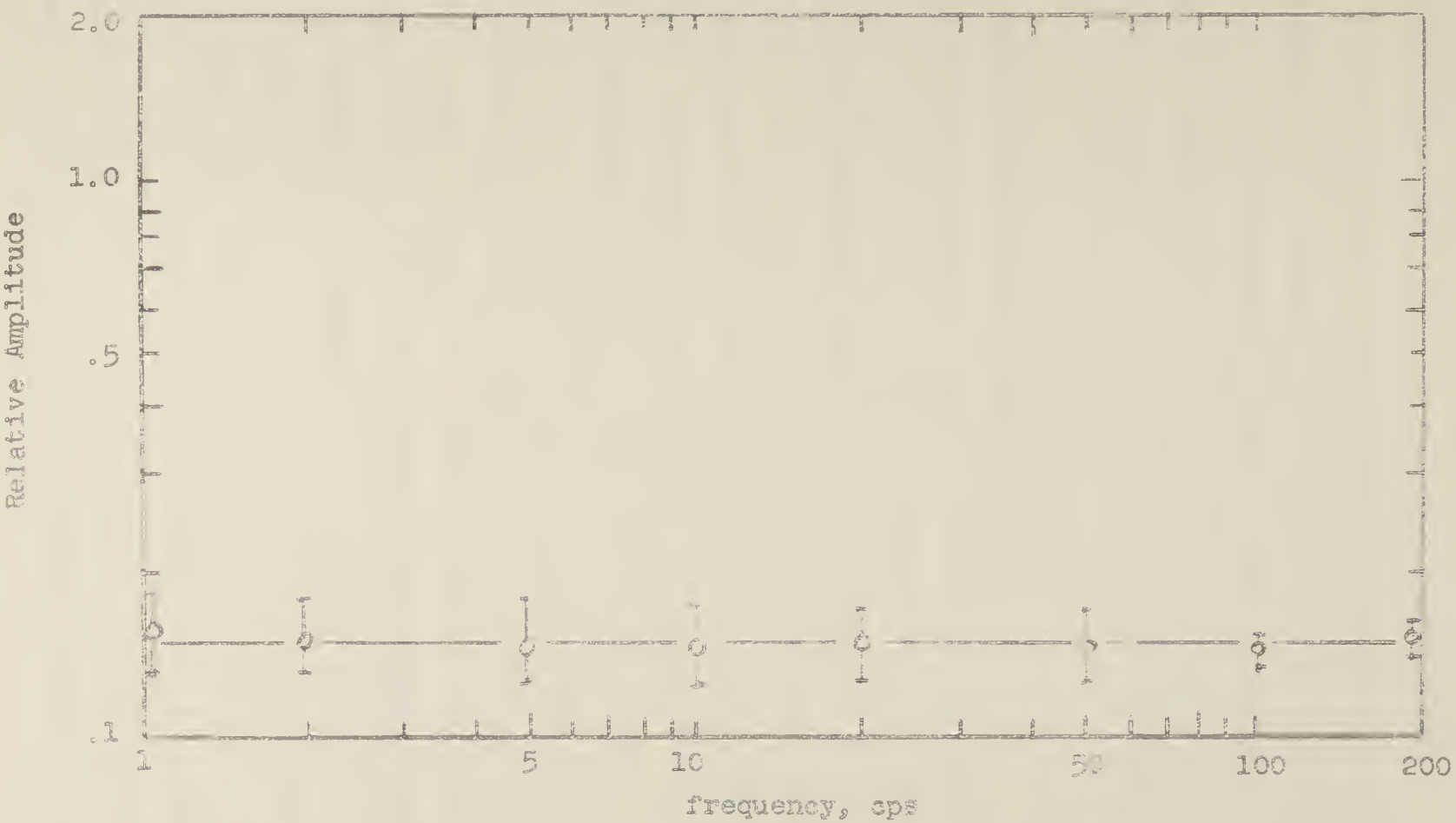

Fig. 3.3 Low-Frequency Hohlraum Measurements
After Modifying Equipment

$$f = \frac{1}{2\pi R_f C_f} = 314 \pm 4 \text{ cps}$$

At the same time, the filters were modified to widen the pass band, which would allow shorter integration times (see Appendix D). The filter modifications are shown in Fig. 3.4.

Results of the simulated lattice measurement are shown in Fig. 3.5. The breakpoint occurs at that frequency corresponding to a 6 db decrease in the squared signal and is estimated to be 320 ± 20 cps, which is in good agreement with the predicted value of 314 ± 4 cps.

3.3 Lattice Autocorrelation Measurements

Having been satisfied that the system was now functioning properly, attention was turned to making a test run in a D_2O-moderated, uranium-fueled lattice. Estimates of k_{eff} and α for the lattice installed in the exponential facility during this thesis work are developed in Appendix C, indicating that a detector efficiency of around 30% would be required to enable determination of α for this particular lattice. Nonetheless, since it would be several months at least until a more reactive lattice was scheduled for installation, it was decided to make a test run to insure that the equipment would be ready for use. These measurements were made by suspending the 6377 boronlined detector in a lead-weighted aluminum tube in the center of the lattice core. In order to do this, the seven center fuel rods had to be removed from the 211 rod lattice. Since the multiplication factor of the assembly was already so low as to preclude measurement of kinetic effects, the small additional decrease in reactivity caused by removing

Switches:

Position "HI"

$$\frac{e_o}{e_i} = - \frac{20s}{(1+10s)(1+.02s)}$$

Position "LO"

$$\frac{e_o}{e_i} = - \frac{200s}{(1+10s)^2}$$

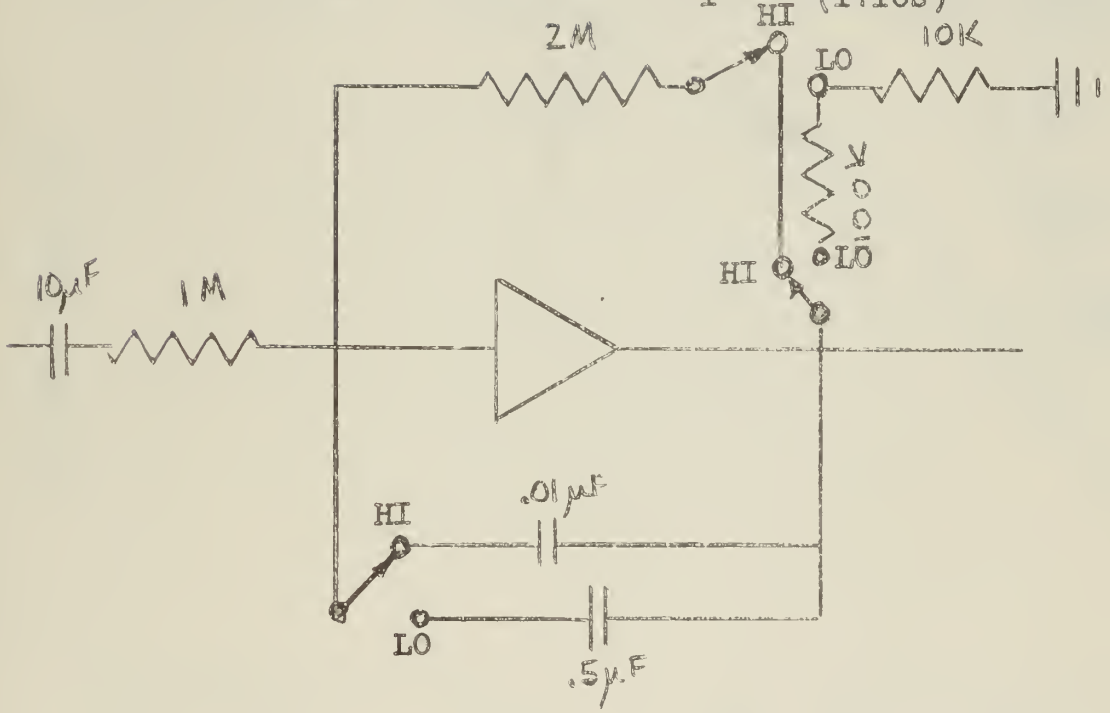

Fig. 3.4 Filter Circuitry Modifications Showing Wide (~10 cps) and Narrow (~0.3 cps) Bandpass Capability

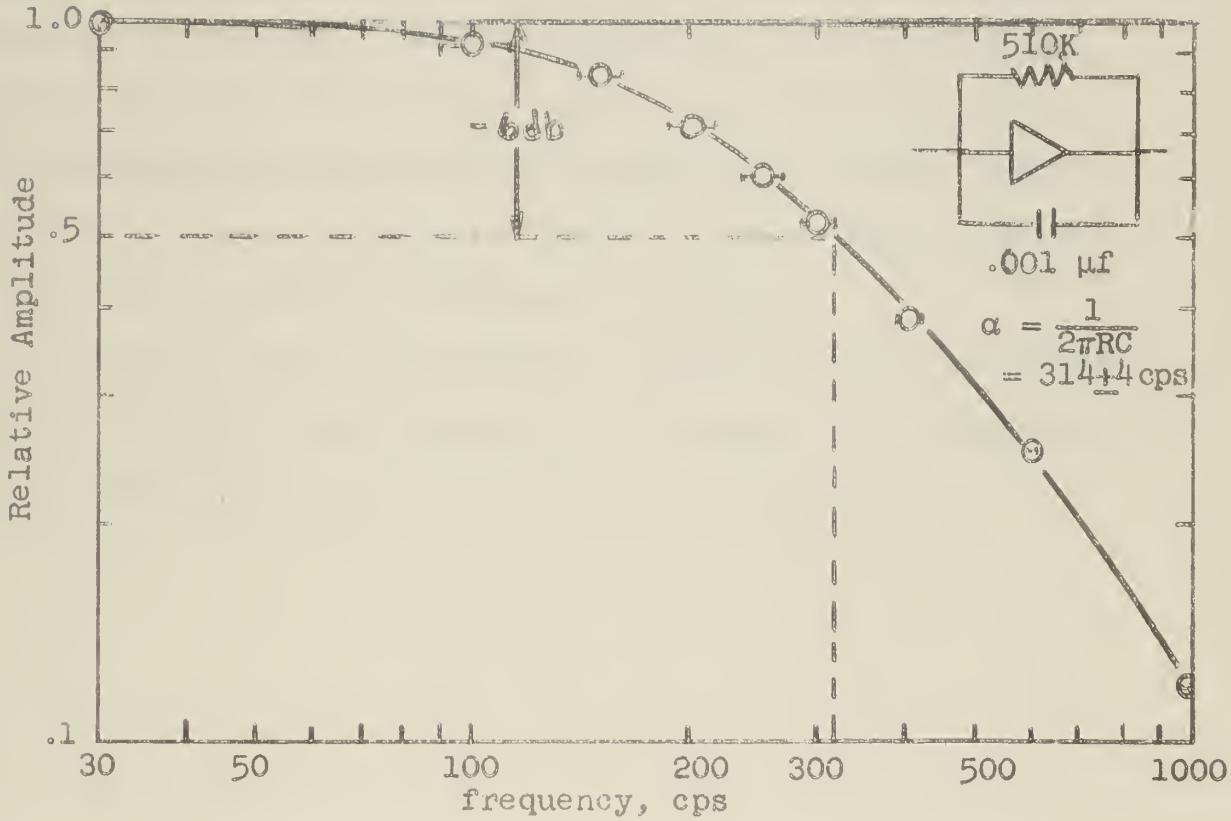

Fig. 3.5 Experimental Determination of Simulated Breakpoint

the rods was not considered significant. First attempts at taking measurements revealed that the 75 foot cable from the detector to the preamp caused excessive oscillation in the preamplifier. Although this oscillation could be eliminated by use of an RC compensating circuit, the signal strength was then so small as to be comparable to the preamp self-noise. Therefore, the preamplifier was placed on the lattice top, eliminating the need for both the long input cables and the compensating network. Such an arrangement produced lattice noise signals five times greater than the preamp self noise. With the equipment set up in this manner, the results shown in Figure 3.6 were obtained. Again, the white-noise spectrum due to the low detector efficiency is evident.

No further work was performed on autocorrelation measurements because the cross-correlation technique to be described in the next chapter appeared to hold more promise.

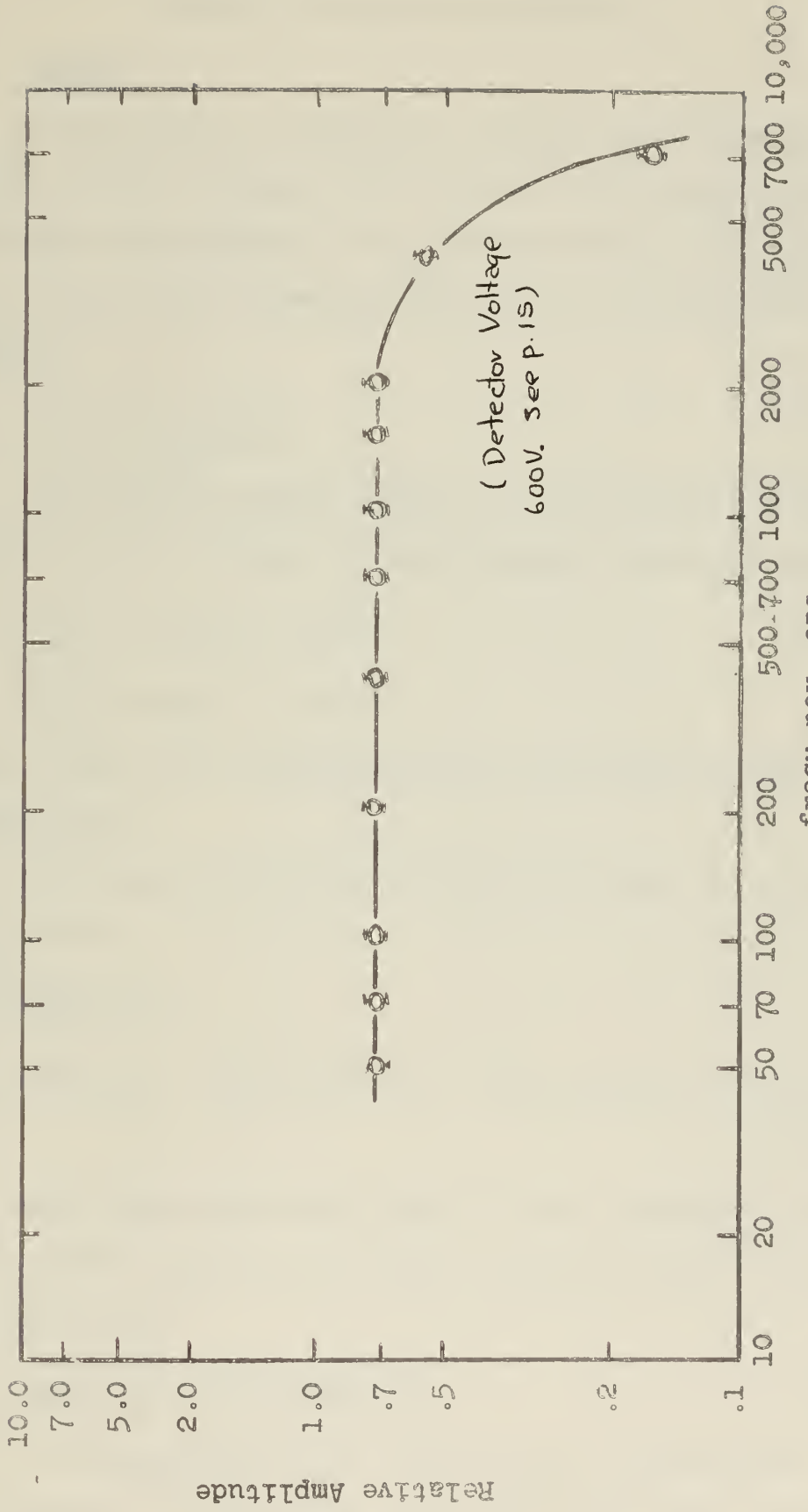

Fig. 3.6 Auto-Spectral Density Measurements in MIT Lattice

CHAPTER 4

CROSS-CORRELATION MEASUREMENTS

4.1 Theory

As mentioned in Chapter 1, cross-correlating the signals should decrease the detector efficiencies needed for noise measurements. The cross-correlation function is defined as the expectation value of two independent signals:

$$E\left[\phi_1(t_1)\phi_2(t_2)\right] \quad . \tag{4.1}$$

Although ϕ_1 and ϕ_2 consist of noise signals superimposed on d.c. levels, we need consider only the noise:

$$\phi_1(t) = U_1(t) + C_1(t) \tag{4.2}$$

$$\phi_2(t) = U_2(t) + C_2(t) \ , \tag{4.3}$$

where U and C are uncorrelated and correlated noise, respectively.

The cross-correlation function of these two signals is given by:

$$E\left[\phi_1(t)\phi_2(t)\right] =$$

$$E\left[U_1(t)U_2(t)\right] + E\left[U_1(t)C_2(t)\right] + E\left[U_2(t)C_1(t)\right] + E\left[C_1(t)C_2(t)\right] \tag{4.4}$$

Since the expectation value of the multiple of two uncorrelated functions is zero, all uncorrelated terms disappear and:

$$E\left[\phi_1(t)\phi_2(t)\right] = E\left[C_1(t)C_2(t)\right] \ . \tag{4.5}$$

Thus, corresponding to Eq. 1.16 for auto-correlation experiments, one can write for cross-correlation experiments:

$$\langle |I_c(\rho)| \rangle^2 = 2\epsilon_1\epsilon_2 F_o Q^2 \frac{\nu(\nu-1)}{(\bar{\nu})^2} k_p^2 \frac{1/\ell^2}{\omega^2 + \alpha^2}, \qquad (4.6)$$

where now ϵ_1 and ϵ_2 refer to the efficiencies of the separate detectors. This would seem to imply that measurements could be made independent of detector efficiency, as long as the analyzer output signal is sufficiently large. However, as stated earlier, Seifritz, et al. found that cross-correlation decreased their efficiency needs only by a factor of 20. This is due to the fact that the cross-terms in Eq. (4.4) are not totally uncorrelated. A factor of 20 reduction in efficiency requirements, however, is a highly desirable, if not essential, improvement if one is to make noise measurements in subcritical systems.

4.2 Equipment

The cross-correlation measurements required the additional equipment shown within the dotted lines in Fig. 4.1, consisting of one additional multiplier (G.A.P. $\pm$ 25 V MU/DV Duplex Multiplier/Divider), 6 operational amplifiers, another preamplifier, and an additional Westinghouse Type 6377 boron-lined ionization chamber.

The two detectors were suspended in the high-flux region of the lattice described earlier, side-by-side, in separate lead-weighted aluminum tubes. Again the preamplifiers were placed on the lattice top, as close to the detectors as possible to avoid preamp oscillations. Both detectors were operated at 670 V.

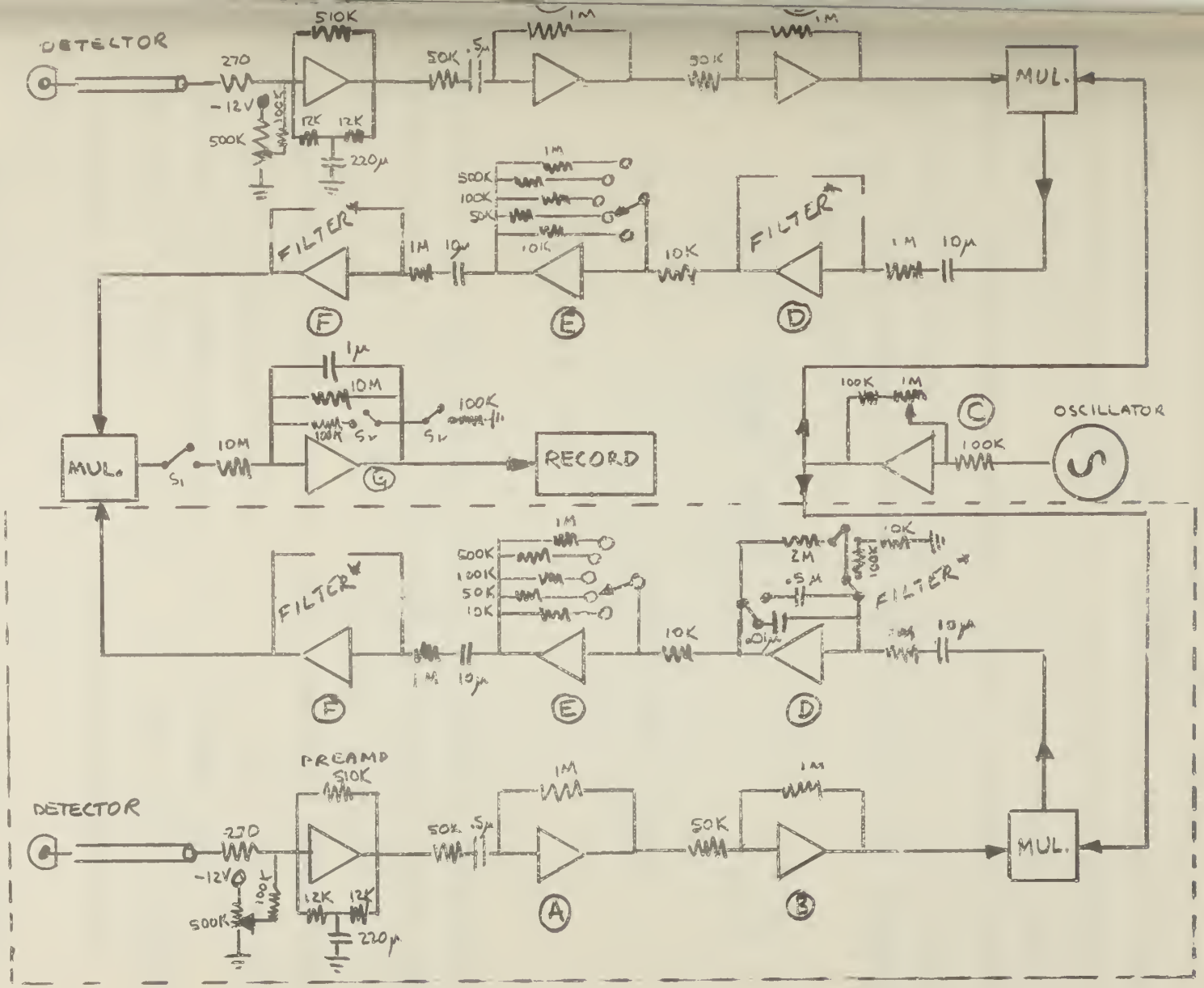

Fig. 4.1 Circuit Diagram for Cross-Correlation Measurements. See App. D for letter designations.* All filters same.

4.3 Results

Recall that for autocorrelation measurements the filtered signal is squared and then averaged. The squaring process naturally results in a large non-~~zero~~ negative signal, whose average will also then be non-~~zero~~ negative. The cross-correlation measurement, in that it eliminates the uncorrelated noise signals, should produce a signal whose magnitude relative to the auto-correlation signal is given by the ratio of Eq. (4.6) to Eq. (1.16). For very low efficiencies, this ratio is merely the right-hand term of Eq. (1.16) and is:

$$\frac{\langle |I_c|^2 \rangle}{\langle |I_a|^2 \rangle} \approx \frac{\epsilon \bar{\nu}(\nu-1)}{(\bar{\nu})^2} \frac{1/\mu^2}{\omega^2 + \alpha^2} k_p^2 \quad . \qquad (4.6)$$

For $\epsilon \approx 10^{-7}$, and for the lattice under study:

$$\frac{\langle |I_c|^2 \rangle}{\langle |I_a|^2 \rangle} \approx 3 \times 10^{-6}$$

Thus since the signal level in the auto-correlation measurements was $\langle |I_a|^2 \rangle \leq 100$ V, the cross-correlation output signal must be $\langle |I_c|^2 \rangle \leq 3 \times 10^{-4}$ V. This signal is so low as to be overridden by equipment drift. While observing this drop in net output confirms predictions as to the effect of converting from auto- to cross-correlation, the low signal made it impossible to extract a spectrum. Even with cross-correlation techniques, therefore, higher lattice multiplications and detector efficiencies will be required.

Experimentation was concluded at this point. Conclusions and recommendations follow in Chapter 5.

CHAPTER 5

SUMMARY, CONCLUSIONS, AND RECOMMENDATIONS

5.1 Summary and Conclusions

A reliable system for making auto- and cross-power noise spectral density measurements on a subcritical nuclear assembly was constructed. The system was demonstrated capable of providing signal analysis over a frequency range of 1 to 5,000 cps.

The assembled system was tested in several applications:

a) a signal simulating a reactor noise spectrum was analyzed to demonstrate successful system performances under optimum operating conditions (Chapter 3, Section 2). The measured breakpoint frequency 320 $\pm$ 20 cps agreed quite well with the known input of 314 $\pm$ 4 cps.

b) The MIT exponential facility hohlraum was studied using the auto-correlation technique. None of the results (Chapter 3, Section 1) gave reason to doubt the assumption that the hohlraum provides a white source of neutrons to the test lattices.

c) Both auto- and cross-correlation measurements were made in a lattice. In both cases it was shown that lattice multiplication and detection efficiencies must be increased before noise analysis can be used to extract neutron decay constants (Chapters 3 and 4).

Since detector efficiency requirements vary inversely as the square of the multiplication factor of the system, future studies should concentrate on lattices with k_{eff} as close to the present lattice safeguard limit of $k_{eff} = 0.9$ as possible. Since cross-correlation of two signals significantly reduces the efficiency requirements, this method provides the greatest promise for successful analysis at reasonable efficiency levels.

5.2 Recommendations

In order to attain the required detector efficiencies, the utility of gamma detectors in the lattice annulus should be fully explored. Such detectors would not disturb the multiplying system, but would detect both prompt fission product gammas, which escaped from the lattice core, and those gammas produced by neutron capture in the cadmium sheath surrounding the lattice. Alternatively it may be possible to develop a detection system which detects the Cerenkov radiation produced in the moderating D_2O. Further, the 2% enriched UO_2 lattices, scheduled for study beginning in February 1967, should provide the capability of attaining $k_{eff} \approx 0.9$, which would also reduce detector efficiency requirements considerably.

Finally, in future work, where large volume detectors must be used, the space dependence of reactor noise measurements should be carefully considered.

APPENDIX A

NOISE-EQUIVALENT SOURCE FOR A SUBCRITICAL ASSEMBLY

Neutron processes in a multiplying system are analogous to the random flow of electrons in a diode. Using this similarity, Cohn has adapted the diode noise equation of Schottky to the noise in a critical reactor.[10] By simple modifications it is possible to extend this treatment to the case of a subcritical system.

Cohn's adaptation of the Schottky formula is:

$$\langle |S_o|^2 \rangle = 2 \sum_i q_i^2 \bar{m}_i \,, \qquad (A.1)$$

where: $\langle |S_o|^2 \rangle$ is the noise-equivalent source;

q_i = net number of neutrons produced in the nuclear process of type i; and

$\bar{m}_i$ = average number of processes of type i occurring per second in the system.

Table A.1 lists the processes, their rate of occurrence, and the net number of neutrons produced in that process.

TABLE A.1

CONTRIBUTIONS TO PILE NOISE SOURCE

Nature of Process	Average Rate of Occurrence	Net Number of Neutrons Produced
Nonproductive leakage or absorption	$\frac{n}{\ell}\frac{A}{A+F}$	-1
Fission giving rise to N prompt neutrons	$\frac{n}{\Lambda}\frac{F}{A+F}P_N$	N-1
External source providing neutrons to maintain the pile	$\frac{n}{\ell}(1-k_p)$	1

In this formulation delayed neutron effects have been neglected. Here

A = macroscopic cross-section for all non-productive processes including leakage,

F = macroscopic cross-section for fission,

n = total number of neutrons in the system,

ℓ = prompt neutron lifetime in sec, and

$\Lambda = \ell/k$ = neutron generation time in sec.

A and F are subject to the neutron balance condition

$$\frac{\bar{\nu} F}{A + F} = k_p \qquad (A.2)$$

where $\bar{\nu}$ is the average number of neutrons produced per fission. P_n is the probability that N prompt neutrons will be produced in any one fission, subject to the conditions

$$\sum_{N=1}^{\infty} P_N = 1 \qquad (A.3)$$

$$\sum_{N=1}^{\infty} N P_N = (1-\beta)\bar{\nu} \simeq \bar{\nu} \qquad (A.4)$$

$$\sum_{N=1}^{\infty} N^2 P_N = (1-\beta)^2 \overline{\nu^2} \approx \overline{\nu^2} \quad . \qquad (A.5)$$

Substitution into Equation (A1.1) yields

$$\langle |S_o|^2 \rangle = \frac{2n}{\ell(A+F)} \left[A+kF \sum_{N=1}^{\infty} (N-1)^2 P_N + (1-k) \right] . \qquad (A.6)$$

Applying conditions (A.3), (A.4) and (A.5) yields

$$\langle |S_o|^2 \rangle = \frac{2n}{\ell} \left\{ \left[1 - \frac{k}{\bar{\nu}} \right] + \left[\frac{k^2}{\bar{\nu}} (\overline{\nu^2} - 2\bar{\nu} + 1) \right] + \left[1-k \right] \right\} . \qquad (A.7)$$

The first term in square brackets is the term due to

nonproductive (e.g., (n,γ) capture and leakage) processes, the second is the term due to fission processes, the third is the term due to the external source. Note that the external source term has been assumed to be frequency independent, and that the entire noise equivalent source is thus a white noise source. Since the fission rate is:

$$F_o = \frac{nk_p}{\bar{\nu}\ell} \quad , \tag{A.8}$$

Eq. (A.7) becomes

$$\langle |S_o|^2 \rangle = \frac{2\bar{\nu}}{k_p} F_o \left[2 - \frac{k_p}{\bar{\nu}} - k_p + \frac{k_p^2}{\bar{\nu}} (\overline{\nu^2} - 2\bar{\nu} + 1) \right]. \tag{A.9}$$

The source neutrons are then correlated by the multiplying process. The correlated component of the noise spectrum is obtained by multiplying equation (A.9) by the nuclear system transfer function:

$$\langle |n(f)|^2 \rangle = |T(f)|^2 \langle |S_o|^2 \rangle$$

$$= \frac{2\bar{\nu}F_o}{k_p} \left[2 - \frac{k_p}{\bar{\nu}} - k_p + \frac{k_p^2}{\bar{\nu}} (\overline{\nu^2} - 2\bar{\nu} + \nu) \right] \frac{1}{\omega^2 + \alpha^2} \tag{A.10}$$

where $\alpha = \frac{1-k_p}{\ell}$ is the prompt neutron decay constant.

The average current $\bar{I}$ in a detector due to all fissions detected will be:

$$\bar{I} = \epsilon Q \frac{nk_p}{\bar{\nu}\ell} = \epsilon Q F_o \tag{A.11}$$

where Q is the charge collected per fission detected. Superimposed on this d.c. level are noise components due to the correlated neutrons and the randomness of the collection process. The former is given by Eqs. (A.10) and (A.11)

$$\langle |I_p|^2 \rangle = \epsilon^2 \frac{Q^2 k_p^2}{(\bar{\nu})^2 \ell^2} \langle |n(f)|^2 \rangle \qquad \text{(A.12)}$$

$$= \frac{2\epsilon^2 Q^2 k_p}{(\bar{\nu})\ell^2} F_o \left[2 - \frac{k_p}{\bar{\nu}} - k_p + \frac{k_p^2}{\bar{\nu}} (\overline{\nu^2} - 2\bar{\nu} + 1) \right] \frac{1}{\omega^2 + \alpha^2} \, . \qquad \text{(A.13)}$$

The latter can be obtained by using the Schottky formula:

$$\langle |I_c|^2 \rangle = 2Q^2 \epsilon F_o \, . \qquad \text{(A.14)}$$

For $\epsilon << 1$, these two terms are first order uncorrelated and are added in quadrature to give

$$\langle |I_a(\omega)|^2 \rangle = 2Q^2 \epsilon F_o \left\{ 1 + \frac{\epsilon k_p}{\bar{\nu}\ell^2} \left[2 - \frac{k_p}{\bar{\nu}} - k_p + \frac{k_p^2}{\bar{\nu}} (\overline{\nu^2} - 2\bar{\nu} + 1) \right] \right\} \frac{1}{\omega^2 + \alpha^2} \, . \qquad \text{(A.15)}$$

This result enables estimation of detector efficiencies needed to extract information from noise signals as shown in Chapter 1, Section 4.

Note that throughout, it has been assumed that the analysis equipment did not introduce any spurious frequency dependence. Such an assumption is justified by the "white" noise spectrum displayed in Figure 3.3.

APPENDIX B

OPERATIONAL AMPLIFIERS AND ANALOG CIRCUITS

An operational amplifier is a high gain amplifier with certain input and output impedances as shown in Figure B.1. Analysis of the circuit shows that:

$$\frac{e_o}{e_i} = - \frac{Z_f}{Z_i} \left[\frac{1}{1 + \frac{1}{A}\left(\frac{Z_f}{Z_i} + 1\right)} \right] , \qquad \text{(B.1)}$$

where Z_f = feedback impedance

Z_i = input impedance

A = open loop gain.

Note that if $A >> \left(\frac{Z_f}{Z_i} + 1\right)$, this reduces to:

$$\frac{e_o}{e_i} \cong - \frac{Z_f}{Z_i} . \qquad \text{(B.2)}$$

Since Z_f and Z_i are complex quantities, various combinations of resistances and capacitances may be used to perform mathematical operations. Table B.1 illustrates the circuits which are used to perform the linear operations in the analyzing equipment.

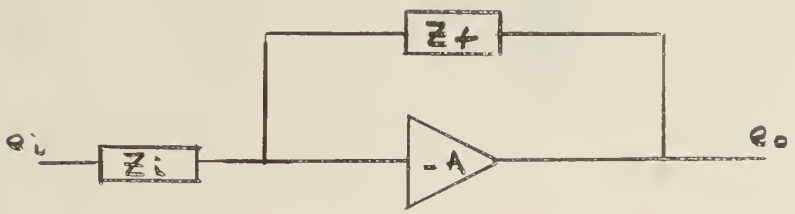

Fig. B.1 Operational Amplifier Circuit

USE	CIRCUIT DIAGRAM	GAIN
SCALER	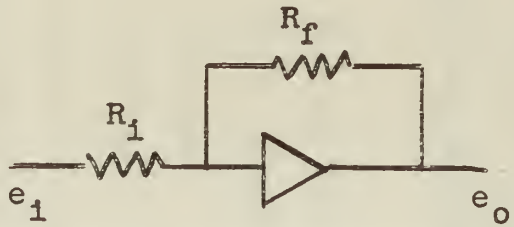	$\frac{e_o}{e_i} = -\frac{R_f}{R_i}$
AVERAGING CIRCUIT	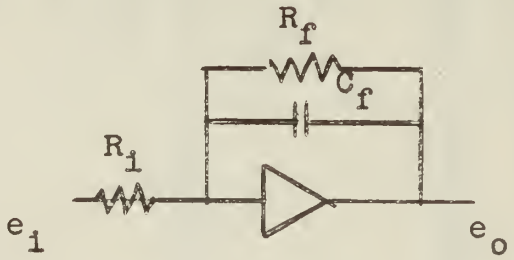	$\frac{e_o}{e_i} = -\frac{R_f}{R_i}\frac{1}{1+R_fC_fs}$
BANDPASS FILTER	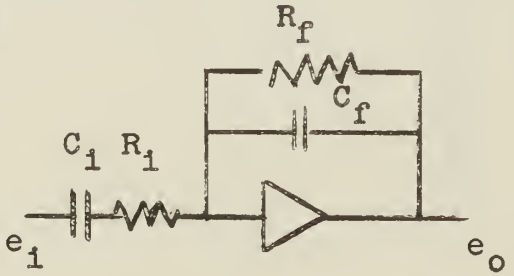	$\frac{e_o}{e_i} = -\frac{R_fC_is}{(1+R_fC_fs)(1+R_iC_is)}$

Table B.1 Circuitry for Basic Linear Operations Employed in Noise Spectral Analyzer

APPENDIX C

ESTIMATION OF k_{eff} AND α

Estimates of k_∞ and α can be made by using the THERMØS computer code.[14] This integral-transport theory code, based on the Wigner-Seitz unit cell model, permits the calculation of:

f_1 the thermal utilization

η the average number of neutrons produced per thermal neutron absorbed in the fuel

$\bar{\Sigma}_a$ the average macroscopic absorption cross-section in the cell

Combining these values with reasonable estimates of:

τ = age to thermal

ϵ = fast fission factor

p = resonance escape probability

$\bar{D}$ = diffusion constant

B_g = geometric buckling,

k_∞ can be estimated by:

$$k_\infty = \frac{(\eta\epsilon pf)\exp(-B_g^2\tau)}{1 + L^2B_g^2} \quad , \qquad (C.1)$$

where $L^2 = \frac{\bar{D}}{\bar{\Sigma}_a}$ = (diffusion length)^2 .

The lattice investigated in the present studies had the following specifications:

Pitch	2.25 in.
Enrichment	0.947% U^{235}
Fuel Density	18.90 gm/cc

D_2O Purity 99.4 MPC

The unit cell dimensions (outer radius minus inner radius) are:

Fuel	0.49149 cm
Air gap	0.00762 cm
Cladding	0.08636 cm
Moderator	2.41491 cm

Using this data, and the procedures outlined in reference (14), the following estimates were derived from the THERMØS output:

$$\bar{\Sigma}_a = 0.007583 \text{ cm}^{-1}$$

$$f = 0.969$$

$$\eta = 1.447$$

For this lattice, good estimates for the other quantities[6] are:

$$\bar{D} \simeq 8.75 \text{ cm}$$

$$p \simeq 0.92$$

$$\epsilon \simeq 1.01$$

$$\tau \simeq 115.4 \text{ cm}^2$$

$$B_g = 0.0031 \text{ cm}^{-2}$$

These values result in:

$$k_{oo} \simeq 1.30$$

$$k_{eff} \simeq 0.65$$

$$\ell \simeq 4.35 \times 10^{-4} \text{ sec}$$

$$\alpha \simeq \frac{1 - k_{eff}}{\ell} \approx 805 \text{ sec}^{-1}$$

Consulting Figure 1.2 one sees that, in this lattice, required efficiencies for successful noise analysis experi-

ments would be:

for autocorrelation: 30%

for cross-correlation 1.5% .

APPENDIX D

COMMENTS ON OPERATION OF EQUIPMENT

D.1 Equipment

The equipment assembled to perform the auto spectral analysis consists of the following (see Figs. D.1 and D.2).

1 George A. Philbrick (GAP) MU/DV Duplex Multiplier Divider - ± 100 V input-output, Ser. 0297

2 GAP Model HK Operational Manifolds, Ser. 069 and 068

8 GAP K2-XA Operational Amplifiers

8 GAP K2-P Stabilizing Amplifiers

8 GAP 2-Unit K-1 Modular Assembly Units

1 Battery Powered A.C. Pre-amplifier utilizing Analog Devices Model 106 Operational Amplifier

2 Associated Specialties Model 2 Power Supply, Ser. 748 and 749

1 Westinghouse Model 6377 Ionization Chamber

10 No. 467 67.5 Volt Batteries

1 Waveforms Model 403B Sine-Square Wave Generator, Ser. 7997

1 Esterline Angus Graphic D.C. Ammeter Model AW, Ser. 85339

Each linear operation is performed using one K2-Xa and one K2-P, which are plugged side-by-side into the top of the manifold. Each manifold can accommodate 5 pairs of these amplifiers. The K-1 Modular Assemblies are labeled to designate which operation is performed. These assemblies are plugged into the face of the HK manifold so as to complete the circuitry for each chopper-stabilized operational amplifier. Each K-1 Assembly is labeled as to input, output, and

Fig. D.1 Auto-Spectral Density Analysis Equipment
(Connecting Cables not Shown)

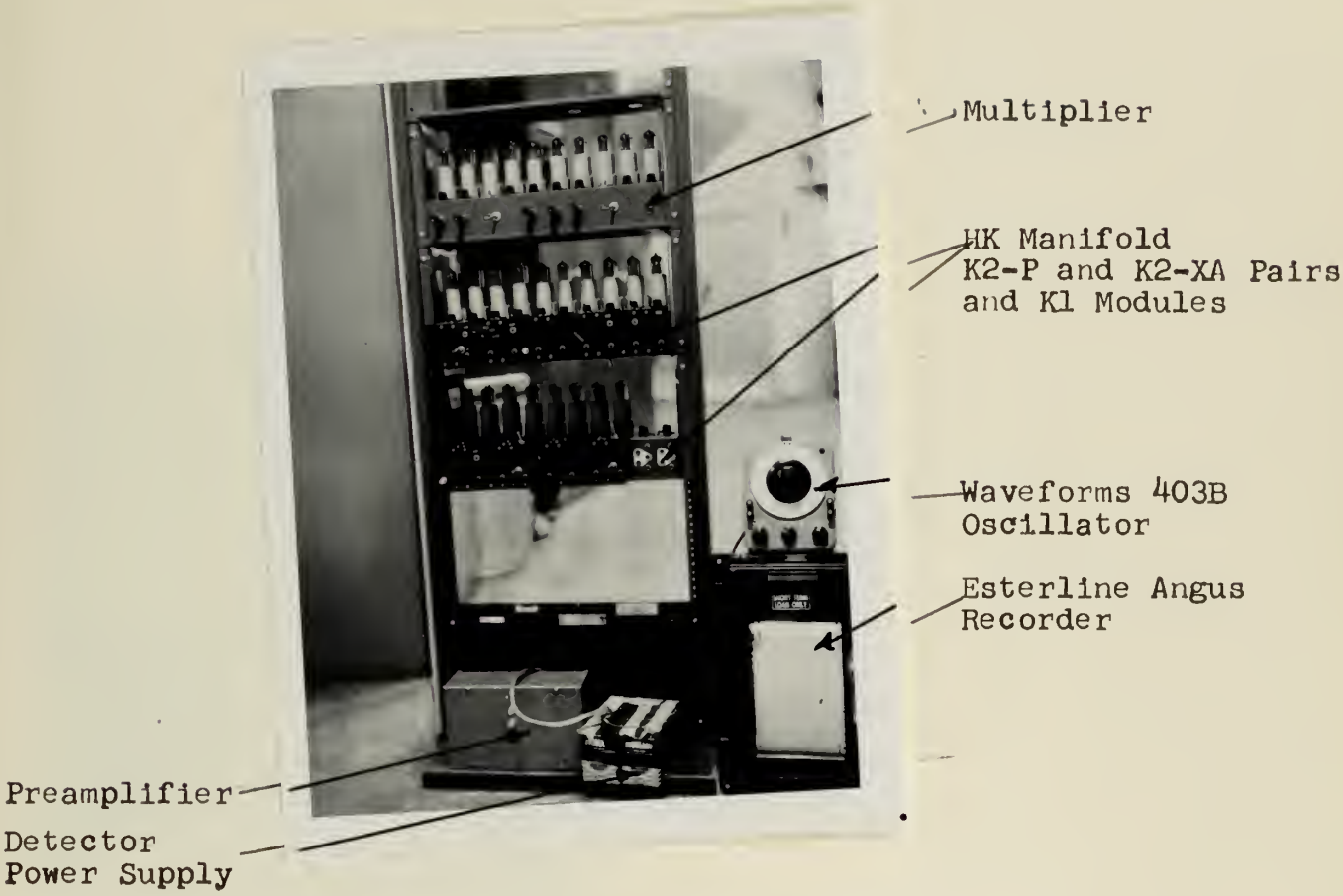

Fig. D.1 Auto-Spectral Density Analysis Equipment
(Connecting Cables not Shown)

Fig. D.2 Photograph Showing Filter Module (Left) - Preamplifier (Right)

ground connections. The eight operations performed are, in order (see Fig. 4.1):

A. Gain of 20 amplification with D.C. blocked

B. Gain of 10 or 20 amplification for noise signal

C. Variable gain (up to 20) amplification for oscillator signal

D. Band pass filter which may be switched to provide either narrow band (~0.3 cps) or wide band (~10 cps) operation

E. Gain of X1, X5, X10, X50, or X100 switchable amplifier

F. Second filter similar to D

G. Averaging circuit

The time constant of the averaging circuit may be altered by using banana plugs to insert various combinations of parallel RC components into the jacks marked FEEDBACK.

In order to perform the cross power spectral measurements, the following equipment was duplicated

detector

preamplifier

detector battery power supply

operational amplifiers and modular units to perform operations A, B, D, E, and F

A $\pm$ 25 V GAP MU/DV Multiplier was borrowed from the MIT Mechanical Engineering Department to serve as the correlating multiplier. A GAP Model R-300 Power Supply was also borrowed to meet the increased power requirements.

D.2 Equipment Operation

In order to insure proper operation, the following had to be observed:

a) Keep equipment well ventilated (e.g. by fan)

b) Maintain largest signal possible throughout without exceeding rated signal input limitations

c) Avoid ground loops

d) Minimize d.c. amplification at preamp by varying resistances in blocking circuit

e) Avoid preamp oscillations by keeping input cables to a minimum length

These comments supplement the individual manufacturer's manuals, which have been included in a booklet Noise Spectrum Analyzer, compiled by the author.

APPENDIX E

PROBABLE ERROR ESTIMATION

E.1 Predicted Error in Amplitude

The spectral measurements are made using an averaging circuit with a time constant $\tau = R_f C_f$ where R_f and C_f are the feedback resistance and capacitance in the averaging circuit. Using formulas developed by van der Ziel[15] and Bendat[16], the relative standard deviation in cross-power spectral density measurements is:

$$\frac{\sigma_{xy}}{S} = \left[\frac{2 + N_1/S + N_2/S + (N_1/S)(N_2/S)}{\pi \Delta f \tau}\right]^{1/2} \qquad (E.1)$$

where S = strength of signal of interest,

$N_{1,2}$ = strength of undesired signals in channels 1 and 2,

Δf = filter bandwidth, in cps, and

τ = averaging circuit time constant.

If detector efficiencies are great enough to detect a level of correlated noise, S and N would refer to the correlated and uncorrelated noise, respectively.

For most measurements in this work, detector efficiencies were so low as to permit measurement of only the uncorrelated signal level. For this case:

$$\frac{\sigma}{S} = \left[\frac{2}{\pi \Delta f \tau}\right]^{1/2} . \qquad (E.2)$$

Preliminary hohlraum measurements were made with

$\Delta f = 0.88 \text{ sec}^{-1}$

$\tau = 100 \text{ sec}$

Final hohlraum and lattice auto-correlation measurements were made with $\Delta f = 10 \text{ sec}^{-1}$

$$\tau = 100 \text{ sec}$$

These result in predicted amplitude errors of 11.9% and 2.5%, respectively, and are considered to be sufficiently small for this work. If in the future, greater accuracy is considered desirable, it may be attained by altering the feedback impedance in the averaging circuit so as to increase $\tau = R_f C_f$.

E.2 Predicted Error in Frequency

Error in frequency measurements arise from the finite bandwidth of the filters and the lack of accuracy in the oscillator dial readings. Frequency resolution due to finite bandwidth is $\pm \Delta f$, and all equipment dial readings are rated to within $\pm 2\%$.

For example, using a filter with a bandwidth of 10 cps to measure the spectral density near a frequency of 300 cps would result in an uncertainty in frequency of ± 10 cps due to finite bandwidth and ± 6 cps due to dial error. This results in a total uncertainty in frequency of ± 12 cps, or about 3.7%. This figure could be reduced by decreasing the filter bandwidth. As can be seen, however, changes in Δf affect both frequency and amplitude uncertainty, thus a choice of Δf should be governed by desired accuracy in both.

REFERENCES

1. "Heavy Water Lattice Research Project Annual Report", NYO-9658, September 30, 1961.

2. "Heavy Water Lattice Research Project Annual Report", NYO-10,208 (MITNE-26), September 30, 1962.

3. "Heavy Water Lattice Research Project Annual Report", NYO-10,202 (MITNE-46), September 30, 1963.

4. "Heavy Water Lattice Research Project Annual Report", MIT-2344-3 (MITNE-60), September 30, 1964.

5. "Heavy Water Lattice Research Project Annual Report", MIT-2344-4 (MITNE-65), September 30, 1965.

6. Bliss, H.E., I. Kaplan, and T.J. Thompson, "Use of a Pulsed Neutron Source to Determine Nuclear Parameters of Lattices of Partially Enriched Uranium Rods in Heavy Water", MIT-2344-7 (MITNE-73), September 1966.

7. Steff, J.R. and R.W. Albrecht, "Space-Dependence of Reactor Noise", Nuclear Science and Engineering, 24, 184-192 (1966).

8. Bierman, S.R., K.L. Garlid and R.W. Albrecht, "Complimentary Use of Pulsed-Neutron and Reactor Noise Measurements", Nuclear Science and Engineering, 22, 206-214 (1965).

9. Thie, J.A., Reactor Noise, Rowman and Littlefield, Inc., New York (1963).

10. Cohn, C.E., "A Simplified Theory of Pile Noise", Nuclear Science and Engineering, 7, 472-475 (1960).

11. Seifritz, W., D. Stegemann and W. Vath, "Two Detector Cross-correlation Experiments in the Fast-Thermal Argonaut Reactor STARK", Int. Symp. on Neutron Noise, Waves, and Pulse Propogation, Gainesville, Florida, February 14-16, 1966.

12. Johnson, M.G., "A Radiation Detector for Noise Analysis on MITR Subcritical Assembly", SM Thesis, MIT (1966).

13. Diez-Moreno, A., "Assembly of a Noise Analyzer for the MITR Reactor", MIT Course 22.42 Laboratory Project, Spring, 1966.

14. Private Communication with M.J. Driscoll, August 1966.

15. Honeck, H.C., "THERMØS, A Thermalization Transport Theory Code for Reactor Lattice Calculations", BNL-5826 (1961).

16. van der Ziel, A., "A Simple Proof of the Formula for the Relative Accuracy of a Noise Power Measurement with a Quadratic Detector", Proceedings of the I.R.E., June 1953.

17. Bendat, J.S., Principles and Applications of Random Noise Theory, Wiley, New York (1958).